Note: This copy is for your personal non-commercial use only. To order presentation-ready copies for distribution to your colleagues or clients, contact us at *www.rsna.org/rsnarights.*

Longitudinal MR Imaging of Iron in Multiple Sclerosis: An Imaging Marker of Disease[1]

Andrew J. Walsh, PhD
Gregg Blevins, MD
R. Marc Lebel, PhD
Peter Seres, MSc
Derek J. Emery, MD
Alan H. Wilman, PhD

Purpose: To investigate the relationship between magnetic resonance (MR) imaging markers of iron content and disease severity in patients with multiple sclerosis (MS) over a 2-year period.

Materials and Methods: This prospective study was approved by the local ethics committee, and written informed consent was obtained from all participants. Seventeen patients with MS and 17 control subjects were examined twice, 2 years apart, by using phase imaging and transverse relaxation (R2*) mapping at 4.7 T. Quantitative differences in iron content in deep gray matter between patients and control subjects were evaluated with repeated-measures multivariate analysis of variance separately for R2* mapping and phase imaging. Multiple regression analysis was used to evaluate correlations of MR imaging measures, both 2-year–difference and single-time measurements, to baseline disease severity.

Results: R2* mapping using 2-year–difference measurements had the highest correlation to disease severity ($r = 0.905$, $P < .001$) compared with R2* mapping using single-time measurements ($r = 0.560$, $P = .019$) and phase imaging by using either single-time ($r = 0.539$, $P = .026$) or 2-year–difference ($r = 0.644$, $P = .005$) measurements. Significant increases in R2* occur during 2 years in the substantia nigra ($P < .001$) and globus pallidus ($P = .035$), which are both predictors of disease in regression analysis, in patients compared with control subjects. There were group differences in the substantia nigra, globus pallidus, pulvinar thalamus, thalamus, and caudate nucleus, compared with control subjects with R2* mapping ($P < .05$), and group differences in the caudate nucleus and pulvinar thalamus, compared with control subjects with phase imaging ($P < .05$).

Conclusion: There are significant changes in deep gray matter iron content in MS during 2 years measured with MR imaging, changes that are strongly related to physical disability. Longitudinal measurements may produce a higher correlation to disease severity compared with single-time measurements because baseline iron content of deep gray matter is variable among subjects.

©RSNA, 2013

[1] From the Department of Biomedical Engineering (A.J.W., R.M.L., P.S., A.H.W.), Division of Neurology (G.B.), and Department of Radiology and Diagnostic Imaging (D.J.E.), Faculty of Medicine and Dentistry, University of Alberta, Edmonton, AB, Canada T6G 2V2. Received February 22, 2013; revision requested April 15; final revision received May 1; accepted May 16; final version accepted May 29. Supported by Canadian Institutes of Health Research and Multiple Sclerosis Society of Canada. A.J.W. supported by a Vanier Canada Graduate Scholarship and an Alberta Innovates Health Solutions MD/PhD studentship. **Address correspondence to** A.H.W. (e-mail: *alan.wilman@ualberta.ca*).

©RSNA, 2013

Brain iron content has been implicated in the pathophysiologic characteristics of multiple sclerosis (MS) and might represent a marker of disease activity or contribute to disease progression (1). Iron content has been studied both histologically and with magnetic resonance (MR) imaging in the deep gray matter and within lesions (2) and could contribute to disease through different mechanisms. MR imaging offers an in vivo approach for analyzing brain iron content and has shown that iron levels are above normal in certain brain regions and that these iron measures in cross-sectional studies correlate with disease severity in MS (3–5). However, the temporal course of brain iron content is unknown, and analysis of iron changes, rather than single-time measurements, could aid in understanding iron pathophysiologic processes in MS or may represent a newer method of classifying disease severity.

Iron is necessary for normal cellular function and is required in DNA synthesis, neurotransmitter production, and adenosine triphosphate generation (6). In many brain regions, iron level increases with age at different rates and there is substantial regional variation (7). Deep gray matter typically contains the highest iron concentration compared with that of other brain regions, possibly because of neurotransmitter metabolism or high energy requirements (8). Although excess iron has been observed in MS, the pathologic process is unclear. Excess or ill-stored iron can cause the formation of free radicals through the Fenton or Haber-Weiss reactions, which can damage proteins, lipids, and DNA (9). Alternatively, iron accumulation may be a by-product of other processes, such as mitochondrial or neuronal dysfunction (6). Whether iron is a contributor to disease or a benign by-product, it could serve as a biomarker of MS disease activity.

Current clinical MR imaging methods for the assessment of MS do not provide quantitative image contrast. Furthermore, many MR imaging methods of evaluating disease severity, such as measuring lesion load or counting new gadolinium-enhancing lesions, do not significantly (P = .32 and .68, respectively) correlate with functional measures (10,11). Longitudinal lesion analyses either show no correlation (10) or a moderate correlation to disability (12,13). Iron measurement of deep gray matter by using MR imaging might provide a method of predicting disease severity and therefore serve as a biomarker for disease progression. There are several MR imaging techniques that are sensitive to iron, including the transverse relaxation rates R2 (14) and R2* (15) and phase imaging (16). These methods indicate increased iron content in patients with MS relative to healthy control subjects in many deep gray matter regions (4,5,17). Furthermore, correlations have been demonstrated between these MR imaging methods and functional measures such as the Kurtzke Expanded Disability Status Scale (EDSS) (4), cognition (18), and disease duration (17). However, the temporal relationship of iron accumulation in relapsing remitting (RR) MS is unknown from cross-sectional MR imaging studies. A wide variation in normal iron content in deep gray matter exists across individuals (7); therefore, single-time iron measurements may not be adequate to determine whether iron content is pathologically changing in individual patients. Longitudinal analysis would be more powerful in distinguishing abnormal brain iron content in individual subjects.

Investigators in previous imaging studies have used nonquantitative, T2-weighted fast spin-echo methods in longitudinal iron analysis (19–21). However, the image contrast generated is dependent on imaging parameters, and that factor makes interstudy comparisons difficult. Furthermore, researchers in these investigations did not compare iron measurements with those in a control group. This point is important, as disease-related iron accumulation must be differentiated from normal age-related accumulation.

Phase imaging and R2* mapping are promising methods for iron

Advances in Knowledge

- Two-year–difference measurements of deep gray matter by using transverse relaxation (R2*) mapping have a high correlation to physical disability in multiple sclerosis (MS) (r = 0.905, P < .001).
- Differences in R2* measured during 2 years have a higher correlation to disease (r = 0.905, P < .001) than single-time measurements (r = 0.560, P = .019).
- R2* mapping of deep gray matter has high intrasubject image–repeat-image reliability (1.8% ± 1.3 [standard deviation] variation).

Implication for Patient Care

- Quantitative iron evaluation of deep gray matter, based on R2* MR imaging measurements, has a high correlation to physical disability and could be useful as a surrogate marker to follow disease disability during short intervals in individuals or populations with MS.

Published online before print
10.1148/radiol.13130474 **Content code:** NR

Radiology 2014; 270:186–196

Abbreviations:
AC-PC = anterior commissure–posterior commissure
EDSS = Expanded Disability Status Scale
MS = multiple sclerosis
ROI = region of interest
RR = relapsing remitting
SS = severity score

Author contributions:
Guarantors of integrity of entire study, A.J.W., G.B., A.H.W.; study concepts/study design or data acquisition or data analysis/interpretation, all authors; manuscript drafting or manuscript revision for important intellectual content, all authors; approval of final version of submitted manuscript, all authors; literature research, A.J.W., G.B., R.M.L.; clinical studies, A.J.W., G.B., R.M.L., P.S., D.J.E., A.H.W.; statistical analysis, A.J.W., A.H.W.; and manuscript editing, all authors

Conflicts of interest are listed at the end of this article.

evaluation in deep gray matter and hold several advantages over other MR imaging methods: Image contrast is less influenced by imaging parameters, imaging times are relatively fast, and data for both image types can be collected in the same sequence. Although many tissue components can influence the image contrast of phase imaging and R2* mapping, iron content contributes substantially in deep gray matter (22,23) and iron sensitivity increases with increasing field strength (24). This study uses these quantitative MR imaging methods to longitudinally evaluate iron accumulation in the deep gray matter in patients with RR MS relative to control subjects. Therefore, the purpose of this work was to longitudinally investigate the relationship between imaging markers of iron content and disease severity in patients with MS over a 2-year period.

Materials and Methods

Subjects

Seventeen patients with RR MS and 17 age- and sex-matched control subjects were studied from June 2009 to December 2012 in this prospective study. Institutional ethical approval and informed consent were obtained from the subjects prior to the study. Each subject was imaged twice, 2 years apart. Inclusion criteria for patients were that they received a diagnosis of RR MS according to the 2005 McDonald criteria (25) and that they were ambulatory without aid (EDSS, <6.0) at the time of enrollment. Exclusion criteria for all subjects were that they had other neurologic diseases or that they had contraindications to MR imaging. None of the patients or volunteers who were enrolled and provided informed consent were subsequently excluded.

MR Imaging Data Acquisition and Processing

Imaging was performed with a 4.7-T MR imaging system (Unity Inova; Varian, Palo Alto, Calif). Three-dimensional multiecho gradient-echo R2* mapping was performed with the following parameters: repetition time, 44 msec; first echo, 2.93 msec; number of echoes, 10; echo spacing, 4.1 msec; flip angle, 10°; field of view, 160.0 × 256.0 × 160.0 mm; voxel size, 1.0 × 1.0 × 2.0 mm; and acquisition time, 9.4 minutes. Two-dimensional flow-compensated single-echo gradient-echo phase imaging was performed with the following parameters: repetition time msec/echo time msec, 1540/15; flip angle, 65°; number of contiguous sections, 50; field of view, 192.5 × 256.0 × 100.0 mm; voxel size, 0.5 × 0.75 × 2 mm; and acquisition time, 6.6 minutes. A volumetric T1-weighted acquisition was also performed to assess head position measured along the anterior commissure–posterior commissure (AC-PC) line in the sagittal orientation.

R2* mapping used a weighted nonlinear least-squares fit to a monoexponential signal decay versus echo time. Prior to fitting, source images were intensity corrected to compensate for large-scale air-tissue susceptibility effects (26); weighting factors were inversely proportional to the intensity correction factor to account for noise amplification. Phase images were processed by using two separate background phase removal methods: a standard high-pass Hanning filter with a filter width of 0.125 (27) and a moving-window gradient fitting with a filter width of 0.0625 (28).

Region-of-Interest Analysis

Region-of-interest (ROI) analysis with the use of ImageJ (29) was conducted by separately obtaining two-dimensional ROIs from axial R2* maps and magnitude images from the phase acquisition. ROIs from R2* maps were subsequently verified on gradient-echo magnitude images (echo time, 15 milliseconds) from the R2* mapping acquisition. Regions studied included the head of the caudate nucleus, putamen, globus pallidus, thalamus (excluding the pulvinar thalamus), pulvinar thalamus, substantia nigra, and red nucleus. The AC-PC angle was obtained in each subject prior to ROI placement and the correct section for each structure was identified in the superior-inferior direction relative to the standard. ROIs were standardized between subjects, on the basis of axial deep gray matter orientation with the AC-PC line oriented at 0°. The standard orientation defines axial ROIs through the center section of the putamen and from the caudate nucleus, globus pallidus, thalamus, and pulvinar thalamus in the same section, and inferiorly, ROIs through the center section of the substantia nigra and through the red nucleus in the same section (Fig 1).

In phase images, the effects of nonlocal external magnetic fields were mitigated by obtaining reference phase measurements from nearby normal-appearing white matter (23) both directly adjacent to each structure and separately in frontal and posterior white matter (Fig 1).

Statistical Analysis

MR imaging markers of iron content were evaluated longitudinally in each structure by using separate repeated-measures multivariate analysis of variance with a Wilks lambda test in SPSS (IBM, Armonk, NY). Parameter values were averaged in each two-dimensional ROI and then were averaged between hemispheres. Group differences were evaluated between subjects with MS and control subjects, as a between-subject effect, and changes over time were evaluated as a within-subject effect.

Multiple regression analysis was conducted to determine the correlation between 2-year changes in deep gray matter iron content and the baseline MS severity score (SS) (30) independently with both phase imaging and R2* mapping measurements. A separate multiple regression analysis was performed to determine whether measurements obtained by using a single time, from the second MR imaging examination in each subject, are an effective predictor of MS SS. For both tests, a backward-elimination model was used with $P = 0.1$ for removal, with seven deep gray matter

Figure 1

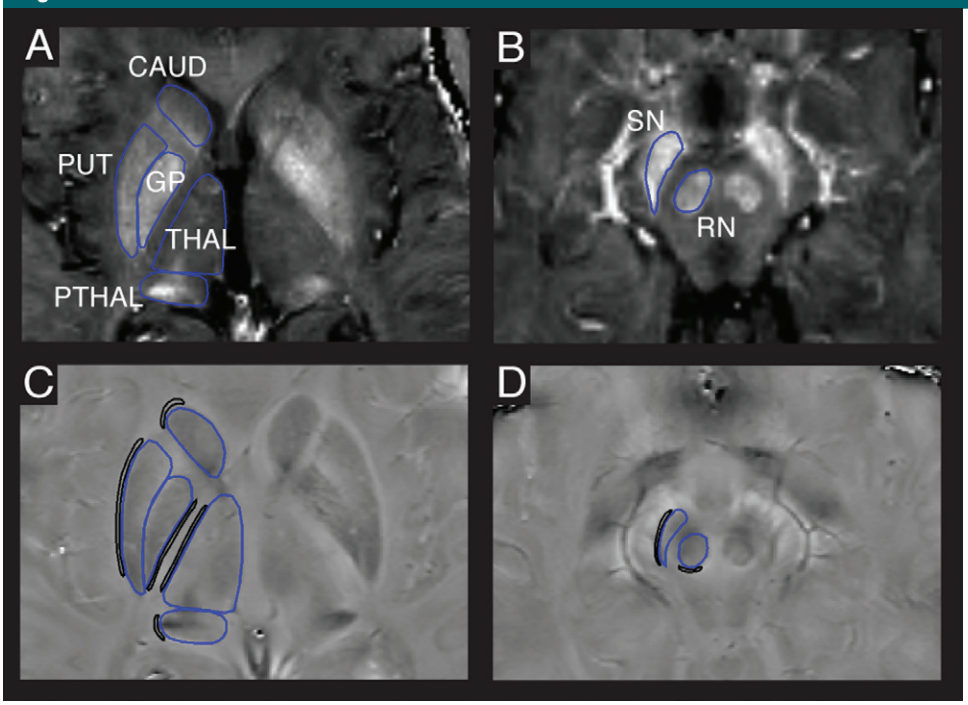

Figure 1: *A, B,* R2* maps (repetition time, 44 msec; first echo , 2.93 msec; number of echoes, 10) show ROI placement (blue outline) for the seven deep gray matter structures in a 36-year-old female patient with MS (EDSS score, 5.0). *C, D,* Corresponding phase images (1540/15). Baseline phase measurements (black outline) are obtained directly adjacent to structures to minimize nonlocal magnetic fields and separately in white matter for reliability comparison for phase images (not shown). *CAUD* = head of caudate nucleus, *GP* = globus pallidus, *PTHAL* = pulvinar thalamus, *PUT* = putamen, *RN* = red nucleus, *SN* = substantia nigra, *THAL* = thalamus excluding the pulvinar thalamus.

regions included as variables (Fig 1). A neurologist who specializes in MS (G.B., with 7 years of experience) measured the EDSS value in each subject. Baseline disability, which was not influenced by an acute relapse, was obtained by measuring the EDSS value close in time to the second MR imaging, fulfilling two criteria: *(a)* EDSS value measured at the time of the study MR imaging if the last relapse occurred more than 4 months before the study MR imaging, or if the last relapse occurred less than 4 months before the study MR imaging and the EDSS value returned to prior baseline level and *(b)* EDSS value measured prior to relapse if relapse occurred less than 4 months before the study MR imaging and EDSS value at the time of the study MR imaging increased from the baseline level. EDSS values and disease duration were input into the MS SS test program (30) to obtain MS SS values.

To establish intrasubject variance of the quantitative MR imaging methods with two-dimensional ROI analysis, a reliability test was performed in four healthy individuals aged 24–50 years who underwent the same MR imaging protocol, twice in the same day.

Results

Subjects

The control subjects, compared with the patients with MS, had no significant differences in age or in the time between the two MR imaging measurements (Table 1). There were no significant differences in head angle, as measured with the AC-PC lines, between patients (mean, 6.0° ± 7.1 [standard deviation]) and control subjects (mean, 3.0° ± 6.8), with P = .29 (paired t test) or differences in the head angle, as measured during 2 years in individual subjects, between patients (mean, 0.96° ± 0.74) and control subjects (mean, 1.21° ± 1.14), with P = .34 (paired t test).

Reliability

In the reliability assessment, the gradient phase processing method with adjacent background phase measurements (28) had the lowest intrasubject variability, compared with the other phase processing methods, and was selected for subsequent phase imaging analysis (Table 2). R2* mapping had substantially lower intrasubject variability, compared with phase imaging.

Iron Differences

The results of the multivariate Wilks lambda test for R2* mapping measurements were significant as a between-subject effect for group (P = .004) and as a within-subject effect for time (P = .017) and for time in terms of group (P = .004), whereas phase imaging measurements were only significant as a between-subject effect for group (P = .037) and not as a within-subject effect for time (P = .094) or for time in terms of group (P = .723). This indicates overall group differences across two measurement times between patients with MS and control subjects by using either phase imaging or R2* mapping, overall changes in R2* over time across groups, and changes between patients with MS relative to control subjects over time by using R2* mapping. For R2* mapping, significant within-subject

Table 1

Subject Demographics

Characteristic	Patients with MS	Control Subjects	*P* Value*
Sex			
No. of female subjects	13	13	. . .
No. of male subjects	4	4	. . .
Mean age (y)†			
Overall	37.1 (27.3–51.4)	36.5 (25.4–54.5)	.38
Male subjects	37.6 (27.3–51.4)	35.3 (27.9–46.5)	.22
Female subjects	37.0 (27.8–50.5)	36.8 (25.4–54.5)	.85
Time between MR imaging and EDSS assessment (wk)‡	106 ± 22	107 ± 23	.24
EDSS score§	2.5 (1.0–6.0)	. . .	. . .
MS SS‡	4.58 ± 2.42	. . .	. . .
Disease duration (y)‖	5.77 ± 2.77	. . .	. . .
Time between MR imaging and EDSS assessment (wk)‡	2.6 ± 7.8	. . .	. . .

* *P* values were obtained by using a repeated-measures Student *t* test.

† Unless otherwise indicated, data are the means, and numbers in parentheses are ranges.

‡ Unless otherwise indicated, data are means ± standard deviations.

§ Data are medians, and numbers in parentheses are ranges.

‖ Disease duration was measured from the index event to the second MR imaging study. Data are the mean ± standard deviation.

Table 2

Same-day Image–repeat-image Test: Percentage of Variation of Deep Gray Matter Measurements by using R2* Mapping, Phase Imaging, and Head Angle

Method	Subject 1	Subject 2	Subject 3	Subject 4
R2* mapping (%)*	1.9 ± 1.3	2.4 ± 1.7	1.8 ± 1.6	1.2 ± 0.8
Phase imaging (%)				
Gradient background phase removal with adjacent background†	10.4 ± 6.3	11.2 ± 8.3	8.4 ± 4.7	7.4 ± 5.0
Gradient background phase removal with distant background‡	19.3 ± 26.1	19.6 ± 22.7	11.0 ± 9.3	27.5 ± 40.5
Standard high-pass filter with adjacent background†	21.6 ± 17.5	14.9 ± 15.1	11.2 ± 8.6	11.3 ± 7.4
Standard high-pass filter with distant background‡	22.4 ± 22.4	17.9 ± 15.6	12.4 ± 13.6	12.4 ± 15.7
Head angle (degrees)				
Image 1	10.0	3.8	−2.6	0.9
Image 2	8.5	4.7	−0.9	0.9

Note.—Measurements were averaged bilaterally in seven deep gray matter structures and then averaged in each subject. Unless otherwise indicated, data are means ± standard deviations.

* Variation in R2* mapping averaged among four control subjects was 1.8 ± 1.3.

† Performed with adjacent background phase measurement.

‡ Performed with frontal and posterior white matter background phase measurement.

effects, using Greenhouse-Geisser tests, showed increases in R2* in patients with MS over time relative to control subjects in the substantia nigra and globus pallidus (Table 3; Figs 2, 3). As between-subject effects, R2* mapping showed significantly larger values in patients with MS, compared with control subjects, in the following five structures: substantia nigra, pulvinar thalamus, thalamus, caudate nucleus, and globus pallidus. Phase imaging measurements showed significant between-subject effects, with lower phase imaging values in patients with MS for only the pulvinar thalamus and caudate nucleus.

Deep Gray Matter Regression to MS SS

By using multiple regression analysis with all deep gray matter structures included as variables, 2-year–difference measurements with R2* mapping had a high correlation to MS SS ($r = 0.905$, $P < .001$). The equation used to predict MS SS was as follows: $\text{MS SS} = 0.232 \cdot \text{ROI}_{SN} - 0.348 \cdot \text{ROI}_{THAL} + 0.279 \cdot \text{ROI}_{GP} + 1.816$, where ROI_{SN} is ROI measurement of the substantia nigra, ROI_{THAL} is ROI measurement of the thalamus, and ROI_{GP} is ROI measurement of the globus pallidus. Substantia nigra, thalamus, and globus pallidus were included in the regression (Fig 4). Two-year–difference measurements with phase imaging correlated to MS SS, with the substantia nigra as a predictor ($r = 0.644$, $P = .005$). The equation used to predict MS SS was as follows: $\text{MS SS} = 0.161 \cdot \text{ROI}_{SN} + 4.465$). Single-time measurements with R2* mapping correlated to MS SS, with the pulvinar thalamus as a predictor ($r = 0.560$, $P = .019$). The equation used to predict MS SS was as follows: $\text{MS SS} = 0.264 \cdot \text{ROI}_{PTHAL} - 4.557$, where ROI_{PTHAL} is the ROI measurement of the pulvinar thalamus. Single-time measurements with phase imaging correlated to MS SS, with the substantia nigra as a predictor ($r = 0.539$, $P = .026$). The equation used to predict MS SS was as follows: $\text{MS SS} = 0.086 \cdot \text{ROI}_{SN} + 6.951$. MS SS was normally distributed across the 17 patients, as measured with the Shapiro-Wilk test ($P = .388$).

Independent regressions showed correlations to MS SS in several structures with R2* mapping and phase imaging, both as single-time measurements and as 2-year–difference measurements. Two-year–difference measurements obtained by using R2* mapping and phase imaging showed that more deep gray matter regions

Table 3

Measurement Differences of Deep Gray Matter Structures between Patients with MS and Control Subjects during 2 Years

	R2* Mapping				Phase Imaging			
Region and Group	Year 0 (sec^{-1})	Year 2 (sec^{-1})	Difference over Time *P* Value	Group Difference *P* Value	Year 0 (ppb)	Year 2 (ppb)	Difference over Time *P* Value	Group Difference *P* Value
Globus pallidus			.035*	.028*			.223	.244
Patient	58.3	62.2			−30.2	−30.1		
Control	56.0	56.7			−29.5	−27.1		
Putamen			.765	.069			.937	.275
Patient	41.2	42.7			−19.0	−20.1		
Control	38.9	39.9			−16.5	−17.6		
Caudate			.311	.033*			.203	.023*
Patient	34.4	35.7			−20.2	−19.1		
Control	32.3	32.0			−16.3	−16.7		
Thalamus			.808	.001*			.837	.25
Patient	28.4	28.4			−14.2	−14.1		
Control	25.5	25.8			−12.9	−12.9		
Pulvinar thalamus			.6	.001*			.59	.043*
Patient	34.3	34.7			−14.8	−15.5		
Control	29.6	29.2			−11.8	−11.9		
Substantia nigra			<.001*	.016*			.843	.225
Patient	53.1	60.2			−26.9	−27.3		
Control	52.3	50.2			−31.8	−31.5		
Red nucleus			.131	.338			.782	.53
Patient	47.8	50.0			−27.0	−27.7		
Control	47.6	47.0			−25.9	−25.9		

Note.— Greenhouse-Geisser tests were used for measurements. ppb = Parts per billion.

* The difference was significant, with $P < .05$.

had a significant correlation to MS SS, compared with single-time measurements, with either MR imaging method (Table 4, Fig 5).

Discussion

In the current study, we demonstrated that longitudinal changes in MR imaging markers of iron content strongly correlated with disability in MS during a short duration of measurement. These changes were relatively large and are above and beyond age-related iron changes.

Ongoing iron accumulation could occur primarily in certain structures during the relapsing remitting stage of disease, as demonstrated by R2* changes in the substantia nigra and globus pallidus. Subdivisions of both of these deep gray matter nuclei serve as output of the basal ganglia and both of these nuclei contain the highest iron concentration in the brain (7). Increased iron concentration in these nuclei in RR MS could arise from different mechanisms, including altered neurotransmitter metabolism of dopamine or glutamate (8); activation of *N*-methyl-D-aspartate receptors, which could enhance iron uptake (31); or altered local energy demands (1).

Multiple regression analysis of R2* mapping to MS SS produced a strong correlation and could provide a new way of following up patients with RR MS over time with imaging. Longitudinal phase imaging and R2* mapping measurements were stronger predictors of MS SS than single-time measurements, possibly because single-time measurements may be insufficient to discriminate elevated iron levels in RR MS from baseline iron variability among subjects (7). Multiple regression analysis may have a higher correlation to MS SS, compared with single regression analysis, as various deep gray matter structures could have iron changes that relate to different aspects of disease. Iron accumulation in structures might not be a slow steady process and could be dynamic with disease progression, as iron could increase in certain structures and decrease in others. Although thalamic iron in patients with MS, compared with that in control subjects, is increased overall, the negative correlation of iron measured in the thalamus to MS SS in the multiple R2* regression might represent iron efflux. A similar iron decrease in the thalamus is observed in healthy individuals between ages 30 and 60 years (7). Phase imaging analysis produces weaker, although still significant, correlations by using either single-time measurements or difference measurements over time, possibly because of the lower reliability of phase imaging. Although phase imaging measurements have been negatively

Figure 2

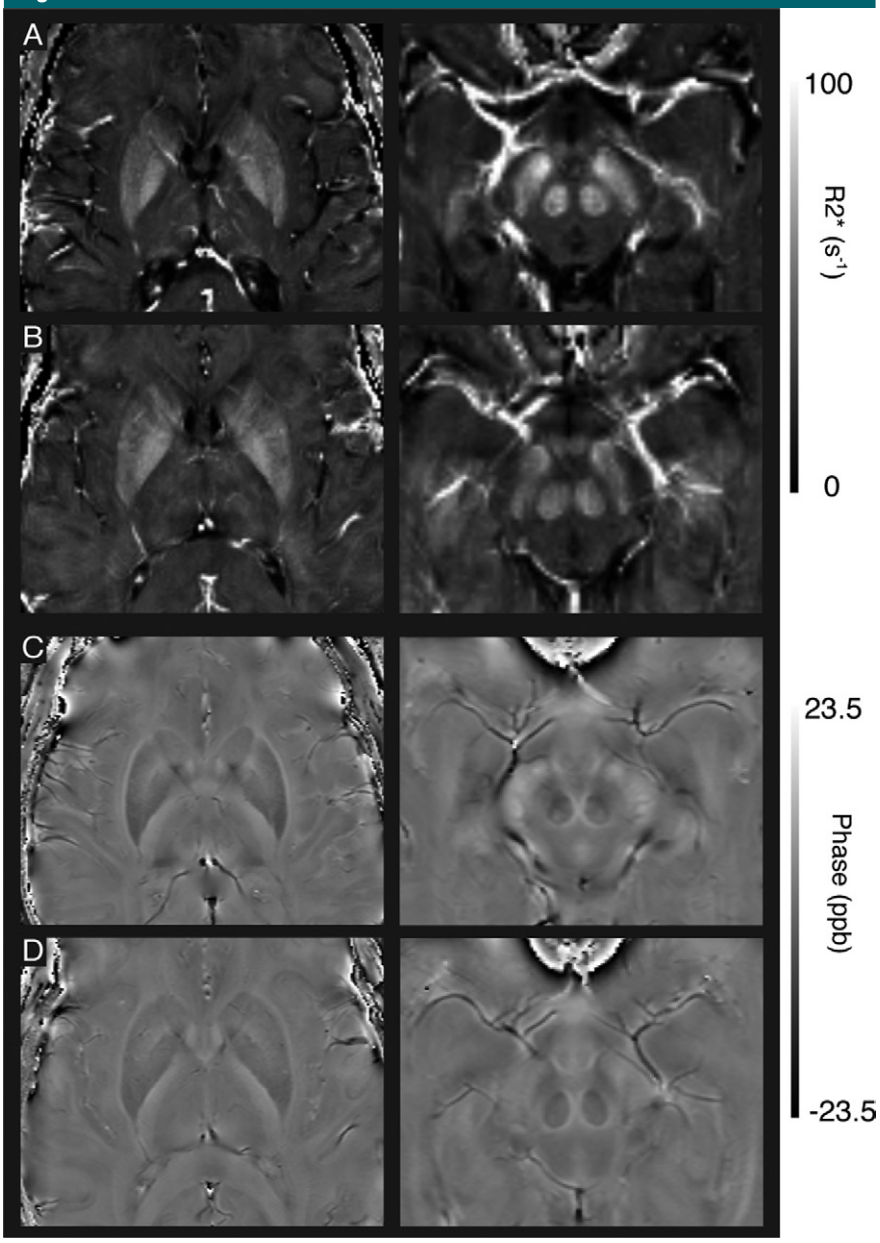

Figure 2: *A, B,* R2* maps (repetition time, 44 msec; first echo, 2.93 msec; number of echoes, 10) and *C, D,* phase images (1540/15) from, *A, C,* a 30-year-old female patient with MS (EDSS score, 1.0) and, *B, D,* a 30-year-old female control subject. The substantia nigra in the patient with MS, compared with the control subject, is more hyperintense in the phase image and R2* map. In the patient with MS, the pulvinar thalamus is more hypointense in the phase image and hyperintense in the R2* map. *ppb* = parts per billion.

correlated with iron in most deep gray matter structures, a positive correlation is observed in the center axial section of the substantia nigra because of shape effects on phase image contrast (32). Because R2* mapping had a high correlation to disease, researchers in future studies could investigate longitudinal R2* measurements for monitoring treatment or for predictive value of disease progression in individual patients. To better understand the biologic process of deep gray matter iron changes in MS, human histopathologic studies or in vitro analysis could offer detailed and specific information.

The intrasubject reliability of phase imaging is lower than that of R2* mapping, possibly because of phase imaging filtering effects with the standard phase imaging method (32) and head-angle differences, which can affect phase imaging measurements (33). Head-angle correction methods or standardization could improve significance and reliability of phase imaging analysis. These issues are less problematic for R2* mapping. Furthermore, differences in the results between phase imaging and R2* mapping could be attributed to physical mechanisms behind image contrast. Phase image contrast depends not only on iron content but also on structure shape, which causes local and nonlocal magnetic fields (32). R2* decay is also affected by other mechanisms, such as dipole-dipole interactions. Multicomponent exponential R2* decay is possible in deep gray matter but is probably more representative of signal decay in highly compartmentalized white matter (34). Furthermore, R2* decay may be nonexponential owing to areas of background magnetic gradients, vascular networks, or a highly compartmentalized iron distribution (35). These factors are likely to be minimal in deep gray matter because a monoexponential model produces a high correlation to iron in both healthy control subjects and patients with MS in validation studies (22,23).

Deep gray matter structures, including the globus pallidus, caudate nucleus, thalamus, pulvinar thalamus, and substantia nigra, showed group differences in R2* measurements between RR MS patients and the control group, and these results agree with results from previous studies (3,4). Therefore, iron concentration within these structures probably increases early in the disease course and may subsequently plateau or slowly increase in regions other than the globus pallidus and substantia nigra. Investigators in some studies have shown differences between subjects

Figure 3

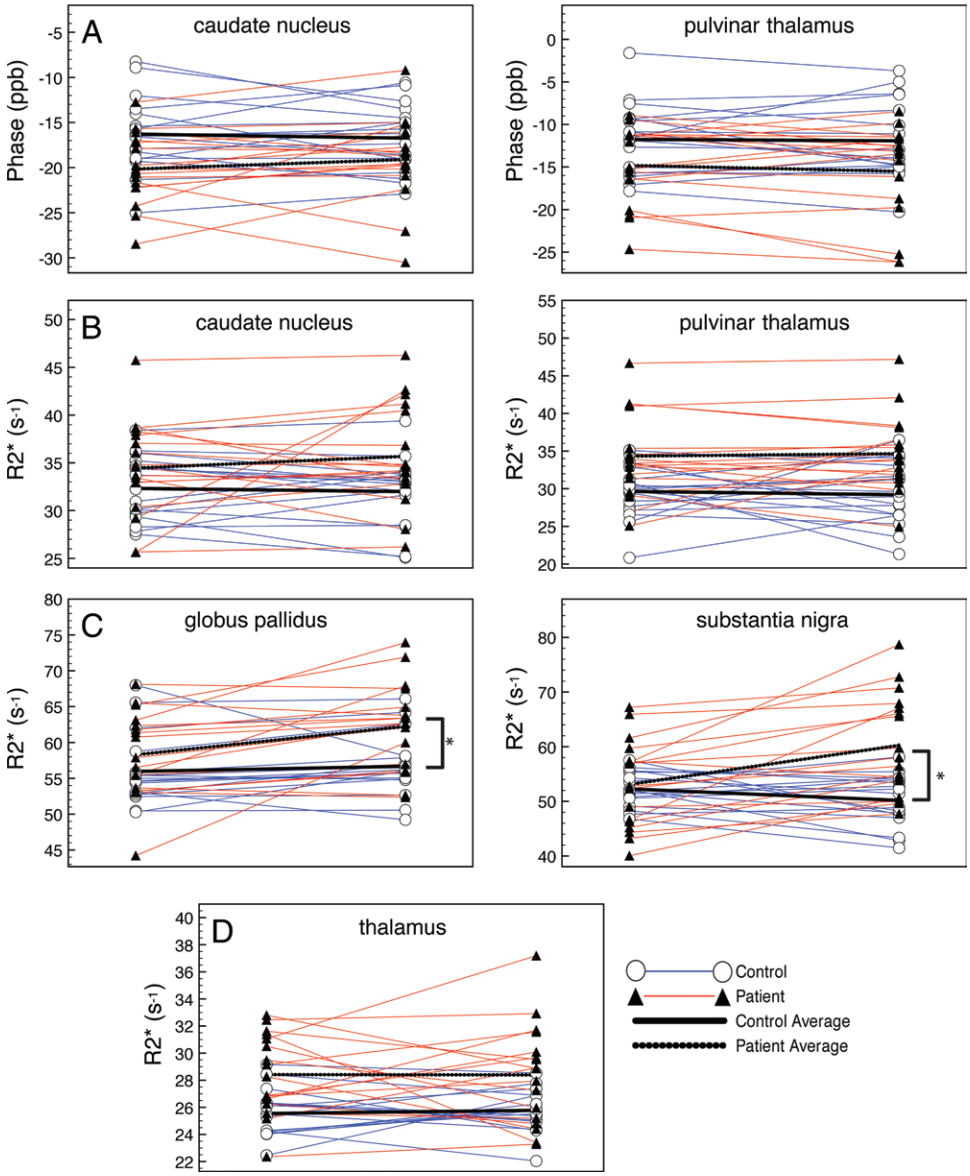

Figure 3: Deep gray matter measurements during 2 years by using, *A,* phase imaging and, *B–D*, R2* mapping. Individual subjects and group averages for patients with MS and control subjects. All structures shown have a significant between-group effect ($P < .05$), indicating an overall difference in iron between subjects with MS and control subjects. * = structures with a significant within-subject effect ($P < .05$), indicating a change over time in iron content between subjects with MS and control subjects. *ppb* = parts per billion.

with clinically isolated syndrome and control subjects by using T2 hypointensity measurements (19), yet there is conflicting evidence as to whether the extent of hypointensity, measured at one time, is a predictor of disease severity. In MS, the caudate nucleus, thalamus, and pulvinar thalamus could have early iron changes caused by axonal degeneration from cumulative damage during acute inflammation. These nuclei have more extensive anatomic connections throughout the cerebrum and brainstem, compared with other deep gray matter nuclei. Iron changes in MS measured with phase imaging may require larger groups to find equivalent significance to R2* mapping differences with smaller groups, as evident in other studies (4,17) that have shown phase imaging differences in additional deep gray matter structures. Iron changes could occur in white matter; however,

Figure 4

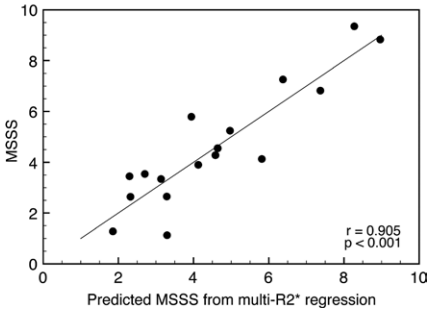

Figure 4: Predicted MS SS *(MSSS)* by using R2* multiple regression analysis compared with measured MS SS. Two-year R2*–difference measurements from substantia nigra, globus pallidus, and thalamus are included in the regression model.

Table 4

Correlation of Deep Gray Matter Structures to MS SS

	2-Year–difference Measurement		Single-time Measurement	
Structure	R2* Mapping	Phase Imaging	R2* Mapping	Phase Imaging
Substantia nigra	0.715 (.001)*	0.644 (.005)*	0.345 (.175)	0.539 (.026)*
Red nucleus	0.317 (.215)	-0.521 (.032)*	0.363 (.153)	−0.259 (.315)
Pulvinar thalamus	0.484 (.049)*	-0.506 (.038)*	0.560 (.019)*	−0.247 (.339)
Thalamus	−0.151 (.562)	−0.375 (.138)	0.004 (.987)	0.260 (.313)
Caudate nucleus	−0.044 (.868)	0.088 (.736)	0.210 (.418)	0.137 (.6)
Putamen	0.045 (.862)	−0.049 (.851)	0.160 (.541)	0.038 (.885)
Globus pallidus	0.484 (.049)*	−0.333 (.192)	0.247 (.34)	−0.028 (.915)

Note.—Data are *r* values, and numbers in parentheses are *P* values.

* The correlation was significant, with $P < .05$.

image contrast in both phase images and R2* maps is more complex in white matter compared with deep gray matter and may require advance-processing techniques to assess tissue iron (36).

The correlation of iron measurements in deep gray matter to disease severity is superior to the correlation of lesion volume changes to disease severity (10,12,13). Iron concentration in deep gray matter may represent global central nervous system dysfunction, while focal white matter hyperintensity can represent local aspects of the disease, including both dysfunction and repair. Gray matter atrophy measurements have been used to show group differences between patients with MS and control subjects, with moderate correlation to disease. However, average gray matter volume changes are small at approximately 0.3%–1.1% per year (37,38), compared with 3.3%–6.7% per year for iron marker changes in the globus pallidus and substantia nigra; and therefore, atrophy may not be as powerful as a biomarker of disease progression in individual subjects or in population studies of shorter duration. In addition, atrophy measures require precise definition of structural borders, which may be ill-defined, while R2* mapping is less dependent on precise edge determination.

There were several limitations with this work. More longitudinal studies, with multiple times and various disease severities, are needed to clarify temporal iron accumulation in specific deep gray matter structures. Measurements in early disease could distinguish which structures are the first to show iron changes with MR imaging; however, the rate of regional iron accumulation in MS might vary, depending on disease duration and disease subtype. In this study, we used a field strength of 4.7 T, which has the benefit of high iron sensitivity; however, there were several limitations. It remains to be determined whether progression of disease would be as well correlated with different field strengths. As well, T1-weighted images have poor deep gray matter contrast at a high field strength, mainly because of longer tissue T1 relaxation times (39). This makes atrophy measurements determined on the basis of current automatic segmentation methods, such as the model-based segmentation and registration tool (Functional MRI of Brain's Integrated Registration and Segmentation Tool, FIRST; FSL, Oxford, England), unreliable at 4.7 T. Longitudinal atrophy measurements in relation to MR imaging measures of iron require further investigation, as iron increases measured with R2* mapping could be in part due to volume reduction (3). However, R2* changes in deep gray matter are greater than atrophy changes, indicating that other factors are likely to be involved. A stepwise multiple regression method was used in this work; however, other methods could be used to evaluate different combinations of predictors, which could yield different results.

MR imaging markers of iron in deep gray matter are easily measurable and show significant and substantial changes during 2 years that strongly correlate with disease severity. R2* mapping and phase imaging measurements compared during 2 years are a more effective predictor of disease severity than single-time measurements. In conclusion, R2* mapping has a strong correlation to disease and a high intrasubject reliability; therefore, this method could be useful as a surrogate marker to follow disease disability during short intervals in individuals or populations with MS.

Disclosures of Conflicts of Interest: A.J.W. No relevant conflicts of interest to disclose. **G.B.** No relevant conflicts of interest to disclose. **R.M.L.** Financial activities related to the present article: none to disclose. Financial activ-

Figure 5

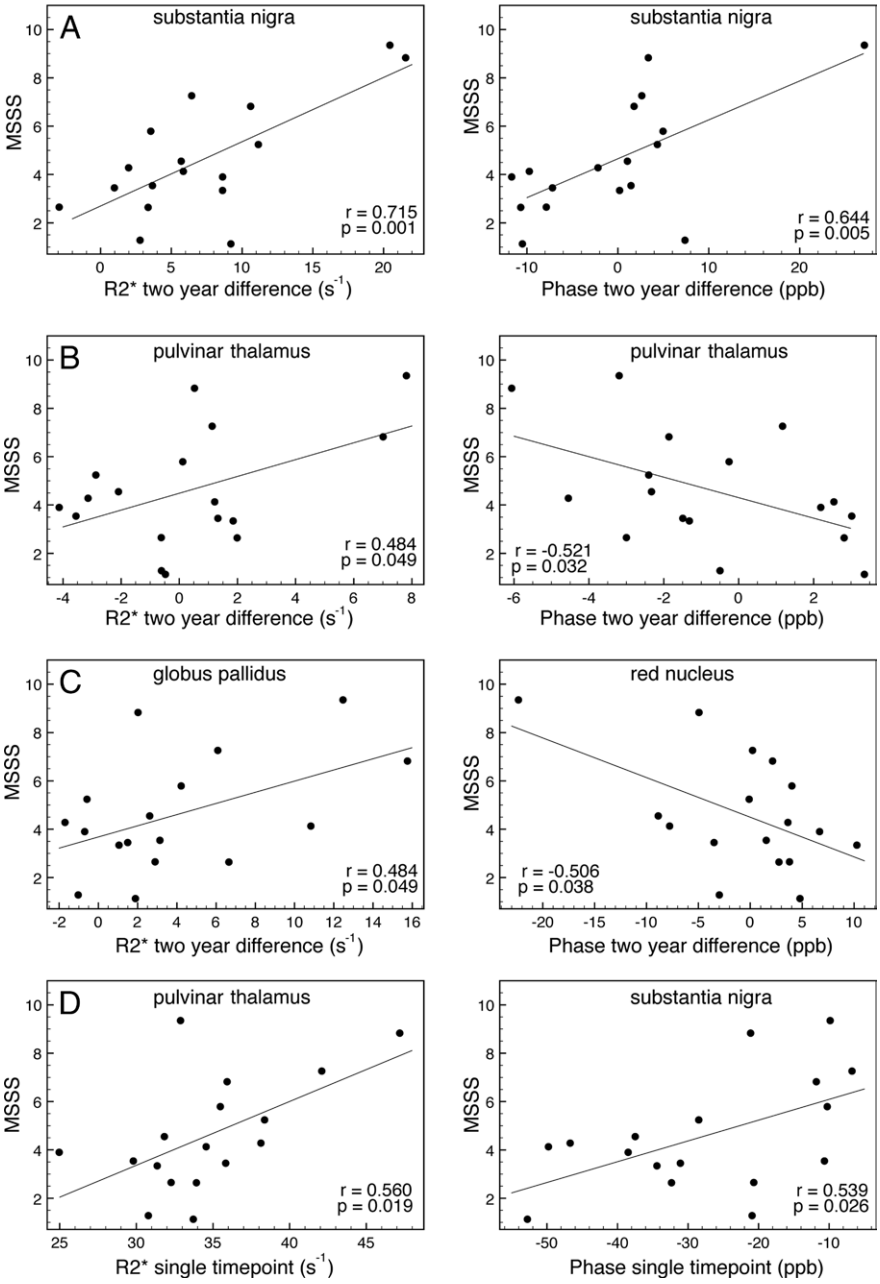

Figure 5: Regressions of deep gray matter MR imaging to MS SS *(MSSS). A–C,* left: Two-year differences with R2* mapping measurements. *A–C,* right: Two-year differences with phase imaging measurements. *D,* Single-time measurements by using R2* mapping (left) and phase imaging (right). *ppb* = parts per billion.

ities not related to the present article: employment by GE Healthcare. Other relationships: none to disclose. **P.S.** No relevant conflicts of interest to disclose. **D.J.E.** No relevant conflicts of interest to disclose. **A.H.W.** No relevant conflicts of interest to disclose.

References

1. Williams R, Buchheit CL, Berman NE, LeVine SM. Pathogenic implications of iron accumulation in multiple sclerosis. J Neurochem 2012;120(1):7–25.
2. Bagnato F, Hametner S, Yao B, et al. Tracking iron in multiple sclerosis: a combined imaging and histopathological study at 7 Tesla. Brain 2011;134(pt 12):3602–3615.
3. Khalil M, Langkammer C, Ropele S, et al. Determinants of brain iron in multiple sclerosis: a quantitative 3T MRI study. Neurology 2011;77(18):1691–1697.
4. Lebel RM, Eissa A, Seres P, Blevins G, Wilman AH. Quantitative high-field imaging of sub-cortical gray matter in multiple sclerosis. Mult Scler 2012;18(4):433–441.
5. Zhang Y, Zabad RK, Wei X, Metz LM, Hill MD, Mitchell JR. Deep grey matter "black T2" on 3 tesla magnetic resonance imaging correlates with disability in multiple sclerosis. Mult Scler 2007;13(7):880–883.
6. Benarroch EE. Brain iron homeostasis and neurodegenerative disease. Neurology 2009; 72(16):1436–1440.
7. Hallgren B, Sourander P. The effect of age on the non-haemin iron in the human brain. J Neurochem 1958;3(1):41–51.
8. Drayer B, Burger P, Hurwitz B, Dawson D, Cain J. Reduced signal intensity on MR images of thalamus and putamen in multiple sclerosis: increased iron content? AJR Am J Roentgenol 1987;149(2):357–363.
9. Meguro R, Asano Y, Odagiri S, Li C, Shoumura K. Cellular and subcellular localizations of nonheme ferric and ferrous iron in the rat brain: a light and electron microscopic study by the perfusion-Perls and -Turnbull methods. Arch Histol Cytol 2008; 71(4):205–222.
10. Miki Y, Grossman RI, Udupa JK, et al. Relapsing-remitting multiple sclerosis: longitudinal analysis of MR images—lack of correlation between changes in T2 lesion volume and clinical findings. Radiology 1999;213(2): 395–399.
11. Kappos L, Moeri D, Radue EW, et al. Predictive value of gadolinium-enhanced magnetic resonance imaging for relapse rate and changes in disability or impairment in multiple sclerosis: a meta-analysis. Gadolinium MRI Meta-analysis Group. Lancet 1999; 353:964–969.
12. Brex PA, Ciccarelli O, O'Riordan JI, Sailer M, Thompson AJ, Miller DH. A longitudinal study of abnormalities on MRI and disability from multiple sclerosis. N Engl J Med 2002; 346(3):158–164.
13. Rudick RA, Lee JC, Simon J, Fisher E. Significance of T2 lesions in multiple sclerosis: a 13-year longitudinal study. Ann Neurol 2006; 60(2):236–242.

14. Gelman N, Gorell JM, Barker PB, et al. MR imaging of human brain at 3.0 T: preliminary report on transverse relaxation rates and relation to estimated iron content. Radiology 1999;210(3):759–767.

15. Haacke EM, Cheng NY, House MJ, et al. Imaging iron stores in the brain using magnetic resonance imaging. Magn Reson Imaging 2005 23(1):1–25.

16. Ogg RJ, Langston JW, Haacke EM, Steen RG, Taylor JS. The correlation between phase shifts in gradient-echo MR images and regional brain iron concentration. Magn Reson Imaging 1999;17(8):1141–1148.

17. Hammond KE, Metcalf M, Carvajal L, et al. Quantitative in vivo magnetic resonance imaging of multiple sclerosis at 7 Tesla with sensitivity to iron. Ann Neurol 2008;64(6):707–713.

18. Brass SD, Benedict RHB, Weinstock-Guttman B, Munschauer F, Bakshi R. Cognitive impairment is associated with subcortical magnetic resonance imaging grey matter T2 hypointensity in multiple sclerosis. Mult Scler 2006;12(4):437–444.

19. Neema M, Arora A, Healy BC, et al. Deep gray matter involvement on brain MRI scans is associated with clinical progression in multiple sclerosis. J Neuroimaging 2009;19(1):3–8.

20. Zhang Y, Metz LM, Yong VW, Mitchell JR. 3T deep gray matter T2 hypointensity correlates with disability over time in stable relapsing-remitting multiple sclerosis: a 3-year pilot study. J Neurol Sci 2010;297(1–2):76–81.

21. Bermel RA, Puli SR, Rudick RA, et al. Prediction of longitudinal brain atrophy in multiple sclerosis by gray matter magnetic resonance imaging T2 hypointensity. Arch Neurol 2005;62(9):1371–1376.

22. Langkammer C, Krebs N, Goessler W, et al. Quantitative MR imaging of brain iron: a postmortem validation study. Radiology 2010; 257(2):455–462.

23. Walsh AJ, Lebel RM, Eissa A, et al. Multiple sclerosis: validation of MR imaging for quantification and detection of iron. Radiology 2013;267(2):531–542.

24. Peters AM, Brookes MJ, Hoogenraad FG, et al. T2* measurements in human brain at 1.5, 3 and 7 T. Magn Reson Imaging 2007;25(6):748–753.

25. Polman CH, Reingold SC, Edan G, et al. Diagnostic criteria for multiple sclerosis: 2005 revisions to the "McDonald Criteria." Ann Neurol 2005;58(6):840–846.

26. Du YPP, Jin ZY, Hu YZ, Tanabe J. Multiecho acquisition of MR angiography and venography of the brain at 3 Tesla. J Magn Reson Imaging 2009;30(2):449–454.

27. Haacke EM, Xu Y, Cheng YC, Reichenbach JR. Susceptibility weighted imaging (SWI). Magn Reson Med 2004;52(3):612–618.

28. Walsh AJ, Eissa A, Blevins G, Wilman AH. Susceptibility phase imaging with improved image contrast using moving window phase gradient fitting and minimal filtering. J Magn Reson Imaging 2012;36(6):1460–1469.

29. Rasband WS. ImageJ. Bethesda, Md: U.S. National Institutes of Health, 1997–2011.

30. Roxburgh RH, Seaman SR, Masterman T, et al. Multiple sclerosis severity score: using disability and disease duration to rate disease severity. Neurology 2005;64(7):1144–1151.

31. Cheah JH, Kim SF, Hester LD, et al. NMDA receptor-nitric oxide transmission mediates neuronal iron homeostasis via the GTPase Dexras1. Neuron 2006;51(4):431–440.

32. Walsh AJ, Wilman AH. Susceptibility phase imaging with comparison to R2 mapping of iron-rich deep grey matter. Neuroimage 2011; 57(2):452–461.

33. Schäfer A, Wharton S, Gowland P, Bowtell R. Using magnetic field simulation to study susceptibility-related phase contrast in gradient echo MRI. Neuroimage 2009; 48(1):126–137.

34. Du YP, Chu R, Hwang D, et al. Fast multislice mapping of the myelin water fraction using multicompartment analysis of T2* decay at 3T: a preliminary postmortem study. Magn Reson Med 2007;58(5):865–870.

35. Yablonskiy DA, Haacke EM. Theory of NMR signal behavior in magnetically inhomogeneous tissues: the static dephasing regime. Magn Reson Med 1994;32(6):749–763.

36. Sati P, van Gelderen P, Silva AC, et al. Micro-compartment specific T2* relaxation in the brain. Neuroimage 2013;77:268–278.

37. Dalton CM, Chard DT, Davies GR, et al. Early development of multiple sclerosis is associated with progressive grey matter atrophy in patients presenting with clinically isolated syndromes. Brain 2004;127(Pt 5): 1101–1107.

38. Bendfeldt K, Hofstetter L, Kuster P, et al. Longitudinal gray matter changes in multiple sclerosis—differential scanner and overall disease-related effects. Hum Brain Mapp 2012;33(5):1225–1245.

39. Rooney WD, Johnson G, Li X, et al. Magnetic field and tissue dependencies of human brain longitudinal 1H2O relaxation in vivo. Magn Reson Med 2007;57(2):308–318.